ELSEVIER

Biochimica et Biophysica Acta 1498 (2000) 233–251

BIOCHIMICA ET BIOPHYSICA ACTA

BBA

www.elsevier.com/locate/bba

# $Ca^{2+}$-binding proteins in the retina: from discovery to etiology of human disease[1]

Izabela Sokal [a,2], Ning Li [e,2], Christophe L.M.J. Verlinde [d], Françoise Haeseleer [a], Wolfgang Baehr [e], Krzysztof Palczewski [a,b,c,*]

[a] *Department of Ophthalmology, University of Washington, P.O. Box 356485, Seattle, WA 98195-6485, USA*
[b] *Department of Chemistry, University of Washington, Seattle, WA 98195, USA*
[c] *Department of Pharmacology, University of Washington, Seattle, WA 98195, USA*
[d] *Department of Biological Structure and BioMolecular Structure Center, University of Washington, Seattle, WA 98195, USA*
[e] *Moran Eye Center, University of Utah Health Science Center, Salt Lake City, UT 84112-5330, USA*

Received 11 September 2000; accepted 12 September 2000

**Abstract**

Examination of the role of $Ca^{2+}$-binding proteins (CaBPs) in mammalian retinal neurons has yielded new insights into the function of these proteins in normal and pathological states. In the last 8 years, studies on guanylate cyclase (GC) regulation by three GC-activating proteins (GCAP1–3) led to several breakthroughs, among them the recent biochemical analysis of GCAP1(Y99) mutants associated with autosomal dominant cone dystrophy. Perturbation of $Ca^{2+}$ homeostasis controlled by mutant GCAP1 in photoreceptor cells may result ultimately in degeneration of these cells. Here, detailed analysis of biochemical properties of GCAP1(P50L), which causes a milder form of autosomal dominant cone dystrophy than constitutive active Y99C mutation, showed that the P50L mutation resulted in a decrease of $Ca^{2+}$-binding, without changes in the GC activity profile of the mutant GCAP1. In contrast to this biochemically well-defined regulatory mechanism that involves GCAPs, understanding of other processes in the retina that are regulated by $Ca^{2+}$ is at a rudimentary stage. Recently, we have identified five homologous genes encoding CaBPs that are expressed in the mammalian retina. Several members of this subfamily are also present in other tissues. In contrast to GCAPs, the function of this subfamily of calmodulin (CaM)-like CaBPs is poorly understood. CaBPs are closely related to CaM and in biochemical assays CaBPs substitute for CaM in stimulation of CaM-dependent kinase II, and calcineurin, a protein phosphatase. These results suggest

Abbreviations: CaM, calmodulin; GCAP, guanylate cyclase-activating protein; CaBP, $Ca^{2+}$-binding protein; GC, guanylate cyclase; GFP, green fluorescent protein

* Corresponding author. Fax: +1-206-221-6784; E-mail: palczews@u.washington.edu

[1] The nucleotide sequences reported in this manuscript have been submitted to the GenBank™/EMBL databank with the following accession numbers: short form of human CaBP1, AF169148; long form of human CaBP1, AF169149; short form of bovine CaBP1, AF169150; long form of bovine CaBP1, AF169151; short form of mouse CaBP1, AF169153; long form of mouse CaBP1, AF1691152; human CaBP2, AF169154; bovine CaBP2, AF169155; short form of mouse CaBP2, AF169156; long form of mouse CaBP2, AF169157; human CaBP3, AF169158; human CaBP5, AF169159; bovine CaBP5, AF169160; mouse CaBP5, AF169161; human CaBP2 genomic sequence, AF170811; exons 1, 2-3-4, 5, 6 of human CaBP5 genomic sequence, AF170812, AF170813, AF170814, AF170815, respectively, and exons 1-2, 3-4, 5, 6 of human CaBP3 genomic sequence, AF170816, AF170817, AF170818, AF170815, respectively, and published recently [F. Haeseleer et al. (2000) J. Biol. Chem. 275, 1247–1260].

[2] Contributed equally to this work.


PII: S0167-4889(00)00099-9

that CaM-like CaBPs have evolved into diverse subfamilies that control fundamental processes in cells where they are expressed. 

*Keywords:* Calmodulin; Neuronal $Ca^{2+}$-binding protein; Myristoylation; Retina degeneration; Gene defect

## 1. Introduction

$Ca^{2+}$ ions play an important role in many biological systems [2–5]. Among these, the retina, as part of the brain, serves as a model system to understand more complex neuronal organizations. The multicellular layered organization of the retina, availability of single cell recordings, quantification of light stimuli, and advances in biochemical and genetic methods provide unprecedented opportunities to understand signal transduction events. Progress in understanding of G-protein-coupled receptor systems, and identification of the architecture of neuronal connectivity are only few examples where studies on the retina paved the way in understanding other systems. Another active research area involves regulation of retinal processes by $Ca^{2+}$ and $Ca^{2+}$-binding proteins (CaBPs) (reviewed in [6]).

A great deal has been learned from studies on $Ca^{2+}$ effects of retinal physiology, and in particular, on regulation of phototransduction in photoreceptor cells [7–11]. Several novel subfamilies of CaBPs related to calmodulin (CaM) were discovered including recoverin [12], guanylate cyclase (GC)-activating proteins (GCAPs) [1,13–17], hippocalcin-like CaBPs [18,19], or CaM-like CaBPs [1] (Fig. 1A). Some of these proteins appear to play important functions in the physiology of neurons in other tissues [18–28]. Systematic work on GCAPs over the last 8 years established rapid progress in understanding their physiological function, structural organization, and potential implication in human pathologies (reviewed in [6,11]). Information on CaM-like CaBPs in the retina emerged only recently, and we are only beginning to understand the role of these proteins in various pathways. Both groups of proteins, GCAPs and CaBPs, appear to be related to an ancestral CaM-like CaBP containing four EF hand loops for $Ca^{2+}$-binding. During evolution, selective elimination of one or two EF hand loops led to creation of novel properties and functions (Fig. 1B). In some genes encoding these proteins, point mutations lead to altered functions causing retina disease, an interesting example being GCAP1(Y99C) linked to autosomal cone dystrophy [29].

In this communication, we present data related to two subfamilies of CaBPs, GCAPs and CaBPs, to illustrate the different extend of progress made on the understanding of the role of these proteins in the retinal neurons and in human pathologies.

## 2. Materials and methods

### 2.1. Expression of bovine GC1 in HEK293 cells

Bovine GC1 was expressed in HEK293 cells using the Bac-to-Bac expression system (Life Technologies, Inc.). To replace the baculovirus polyhedrin promoter with the CMV promoter, a fragment *Bgl*II–*Xho*I from the pcDNA3.1 vector (Invitrogen) covering the pCMV promoter was first cloned between the sites *Sna*BI and *Bam*HI of pFastBac, yielding the vector pFastCMV. The coding sequence of bovine GC1, previously subcloned from pSVL-ROS-GC [30] (obtained from Dr. R. Sharma) in pUC19, was then transferred as a fragment *Eco*RI–*Eco*RI in the *Eco*RI site of pFastCMV expression vector. The expression cassette was then transferred into the baculovirus shuttle vector by transposition as described by the manufacturer. After amplification, the recombinant baculoviruses were concentrated by centrifugation at $80\,000 \times g$ for 1 h at 4°C and resuspended in phosphate-buffered saline. HEK293 were then infected with the concentrated recombinant baculoviruses and the expression of recombinant proteins was tested 1 day after infection. The cells were harvested, washed with 10 mM BTP, pH 7.5, containing 100 mM NaCl, and resuspended at $\sim$0.5 mg/ml for the GC assays.

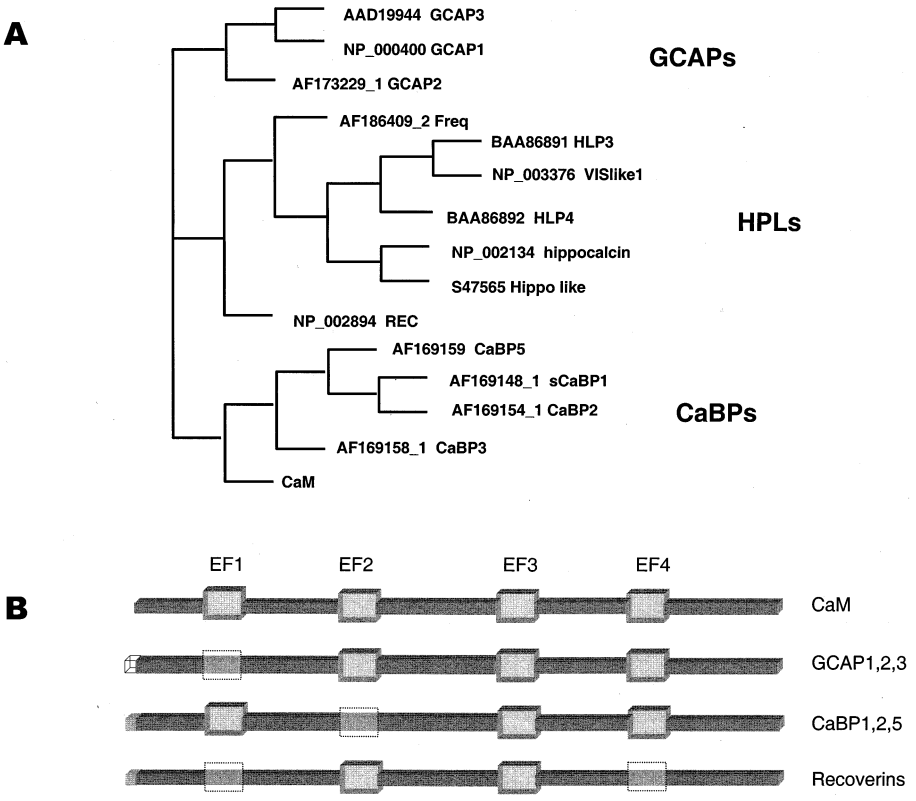


Fig. 1. Phylogenetic analysis and arrangement of functional EF hands in human CaBPs. A: The dendrogram. The figure was generated using Omiga 2.0 (Oxford Molecular) and CLUSTAL W. For analysis, three gene subfamilies were selected, the GCAPs, the hippocalcins/hippocalcin-like proteins (HPL), and CaM-like CaBPs. The accession numbers of respective proteins are followed by an abbreviated name. A sequence alignment of CaM-like CaBPs from various mammalian species is shown in Fig. 5. Abbreviations: FREQ, frequenin; VIS, visinin; REC, recoverin; and CaM. B: Simplified one-dimensional arrangement of functional EF hands in various CaBP subfamilies. Semitransparent boxes represent non-functional EF hands; solid boxes indicate the presence of consensus sequences consistent with $Ca^{2+}$-binding. Presence of a myristoylation site is indicated by an N-terminal box. A filled box indicates presence of a myristoylation site only in some family members.

### 2.2. Expression and purification of bovine and human GCAP1

The bovine GCAP1 coding sequence was amplified by PCR with primers, which inserted $His_6$-tag before the stop codon. The resulting fragment was cloned into pPCR-Script Amp SK(+) (Stratagene). The transfer vector expressing bGCAP1-$His_6$ was constructed by subcloning a *Not*I–*Bam*HI fragment into corresponding sites of the pVL1392 insect cell vector. The transfer vector expressing human GCAP1 (hGCAP1) was constructed as described [31]. High Five insect cells from cabbage looper were transfected with baculovirus vector (pVL1393) carrying the cloned GCAP1 cDNA. Cells were cultured 96 h, homogenized in water containing 2 mM benzamidine and centrifuged at $100\,000 \times g$ for 10 min at 4°C. The supernatant was used as a source of GCAPs. GCAP1 properties were studied from at least two independent preparations. GCAP1-$His_6$ and its mutant proteins used in the GC assays were purified from insect cells on $Ni^{2+}$-nitrilotriacetic acid ($Ni^{2+}$-NTA) columns in non-denaturing conditions according to the manufacturer's protocol (Qiagen). $[Ca^{2+}]_{free}$ was adjusted by EGTA/$Ca^{2+}$ buffer as previously described [32].

### 2.3. Expression and purification of bovine and human GCAP1(P50L)

The P50L mutations were generated in bovine and human GCAP1 with QuikChange™ site-directed mu-

tagenesis kit (Stratagene). The mutagenic primers were: 5′-G AAC CTG AGC CTG TCG GCC AGC CAG (sense) and 5′-CTG GCT GGC CGA CAG GCT CAG GTT C (antisense). All mutant DNA constructs were purified and sequenced as described previously [31]. bGCAP1(P50L) and hGCAP1(P50L) were purified by $Ni^{2+}$-NTA metal affinity chromatography from Qiagen. hGCAP1-(P50L) was purified using G2 affinity chromatography [15,33]. Proteins were purified to apparent homogeneity as determined by sodium dodecyl sulfate–polyacrylamide gel electrophoresis (SDS–PAGE) and Coomassie staining.

### 2.4. Expression and purification of GCAP2-green fluorescent protein (GFP)

The fusion protein GCAP2-GFP (Dr. Iswari Subbaraya, Baylor College of Medicine), GFP fused to the C-terminus of GCAP2, was expressed in Sf9 insect cells and immunoaffinity-purified by a procedure analogous to the purification of GCAP2 [34]. GCAP2-GFP had activating properties indistinguishable from GCAP2 (Subbaraya and Palczewski, unpublished).

### 2.5. GC assays

Washed bovine ROS membranes were prepared from fresh bovine eyes (Schenk Packing Company, Stanwood, WA, USA), reconstituted with recombinant GCAPs and assayed as described previously [15,33]. [$Ca^{2+}$] was calculated using the computer program Chelator 1.00 [32] and in some experiments adjusted to higher concentration by increasing the amount of added $CaCl_2$. The GC assays were performed using [$\alpha$-$^{32}$P]GTP and washed ROS or using recombinant GC1 described previously [15]. The results of GC assays are an average of two determinations. Similar results were obtained from at least two different sets of experiments performed in duplicate. Due to the instability of the GC system (for details, see [15]), the absolute values of one series occasionally varied from another by 10–20%, but with preservation of the ratio between activities of two different preparations (for example, the activity of GCAP1 versus GCAP2). Because only a limited number of the test samples could be performed in a single assay (maximally 24 samples) that always included a relevant control (low, high $[Ca^{2+}]_{free}$ and ± GCAP1), the results are shown without standard deviations.

### 2.6. Cloning of the long and short forms of human CaBP1

Full length CaBPs were amplified by PCR from human, bovine and mouse retina libraries as described previously [1]. The PCR products were cloned. Human CaBP1 was amplified using primers designed based on EST aa363863 (deposited by A.R. Kerlavage, the Institute for Genomic Research, Rockville, MD, USA). The 3′-end was amplified with primers K2 (5′-CTC CGA GAG GCC TTC AGA GAA TTC) and λgt10S (5′-AGC AAG TTC AGC CTG GTA AG). The reaction was cycled through 94°C for 30 s, 68°C for 1 min. The 5′-end was amplified with primers K1 (5′-CCA TCA CCA TTG GTG TCA AAC TCT C) and T7L (5′-GCT CTA ATA CGA CTC ACT ATA GGG) through 35 cycles of 94°C for 30 s, 68°C for 2.5 min. The human CaBP1 short form full coding sequence was amplified with K57 (5′-CAT ATG GGC AAC TGT GTC AAG TAT CC) and K7 (5′-CGG CCT CAG CGG GAC ATC ATC C) through 35 cycles of 94°C for 30 s, 68°C for 1.5 min.

### 2.7. Cloning of bovine CaBP1

The 5′-end of bovine CaBP1 was cloned by PCR with primers K85 (5′-AGC CTC CTT CAT GGA CCC) designed in the 5′-untranslated region (UTR) of hCaBP1 and K81 (5′-TGG CCA CCC AGG TTC ATG TT) designed in the coding region of hCaBP1 through 35 cycles at 94°C for 30 s, 50°C for 30 s and 68°C for 2 min. The 3′-end was amplified by PCR with primers K77 (5′-AAC ATG AAC CTG GGT GGC CA) designed in the coding region of human CaBP1 and K93 (5′-TCG GCG GCT ACA GCG GG) designed in a region of the 3′-UTR of human CaBP1 homologous to the mouse CABP1 3′-UTR through 35 cycles of 94°C for 30 s, 50°C for 30 s and 68°C for 2 min.

### 2.8. Short and long form of human CaBP1

The human CaBP1 full coding sequence was am-

plified with K57 (5′-CAT ATG GGC AAC TGT GTC AAG TAT CC) and K7 (5′-CGG CCT CAG CGG GAC ATC ATC C) through 35 cycles of 94°C for 30 s, 68°C for 1.5 min.

### 2.9. Cloning of mouse CaBP1

The 5′-end of mouse CaBP1 was cycled with K38 (5′-CCC GAA AGG CGT CTC TCA GCT C) and T7L (5′-GCT CTA ATA CGA CTC ACT ATA GGG) through 35 cycles at 94°C for 30 s, 68°C for 2 min. The 3′-end of mouse CaBP1 was cycled with K2 (5′-CTC CGA GAG GCC TTC AGA GAA TTC) and SP6L (5′-GTG AAT TGA ATT TAG GTG ACA CTA TAG) through 94°C for 30 s, 55°C for 30 s and 68°C for 1.5 min.

### 2.10. Cloning of bovine CaBP2

The 5′-end of bovine CaBP2 was cloned by PCR with primers K33 (5′-GTT TAG GCC CAT CAG TTC CAC AA) and T7L (5′-GCT CTA ATA CGA CTC ACT ATA GGG) through 35 cycles of 94°C for 30 s, 60°C for 30 s, 68°C for 2 min. The 3′-end was cloned with primers K50 (5′-CGG CCA GAG GAG ATT GAA GAG) and SP6L through 35 cycles of 94°C for 30 s, 68°C for 2.5 min. The bovine CaBP2 full coding sequence was amplified by PCR on bovine retinal cDNA library with primers K53 (5′-CAT ATG GGA AAC TGT GCC AAG CGG CC) and K8 (5′-TCA GTG ATG GTG ATG GTG ATG GCG GGA CAT CAT CCG GAC AAA C) through 35 cycles of 94°C for 30 s, 56°C for 30 s and 68°C for 2 min.

### 2.11. Cloning of mouse CaBP2

To amplify the 5′-end of mouse CaBP2, 30 PCR cycles of 94°C for 30 s, 68°C for 2 min were run with primers K82 (5′-GCT GCC CGG AGC TCC CCT AC) and T7L (5′-GCT CTA CTC ATA CGA ACT ATA GGG). The 3′-end of mouse CaBP2 was amplified with primers K74 (5′-CAG CAA ATC AGT GGC GGN AA) and SP6L (5′-GTG AAT TGA ATT TAG GTG ACA CTA TAG) through 35 cycles of 94°C for 30 s, 54°C for 30 s and 68°C for 2.5 min.

### 2.12. Cloning of human CaBP2

The 3′-end of human CaBP2 was amplified with primers SP6L (5′-GTG AAT TGA ATT TAG GTG ACA CTA TAG) and K74 (5′-CAG CAA ATC AGT GGC GGN AA) 35 times at 94°C for 30 s, 54°C for 30 s and 68°C for 2.5 min. Part of the 5′-end of human CABP2 was amplified by PCR with primers T7L (5′-GCT CTA ATA CGA CTC ACT ATA GGG) and K75 (5′-CTT CCC GCC ACT GAT TTG CTG) through 35 cycles of 94°C for 30 s, 54°C for 30 s and 68°C for 2 min. The 5′-end of human CaBP2 was obtained through sequencing of a BAC genomic clone covering the human CaBP2 gene.

### 2.13. Cloning of human CaBP3

To amplify the 5′-end of human CaBP3, 35 cycles at 94°C for 30 s, 68°C for 2 min were run with primers K13 (5′-TTT GAC ACG ATT GGA GAT GGG GAG) and λgt10S (5′-AGC AAG TTC AGC CTG GTA AG) and the 3′-end of human CaBP3 with primers K11 (5′-CCT CTG CTT TAA GGG GAT CTG GG) and λgt10S (5′-AGC AAG TTC AGC CTG GTA AG). Primers K11 and K13 were designed based on EST W22993 clone (deposited by Dr. J. Nathans, Johns Hopkins School of Medicine, MD, USA).

### 2.14. Cloning of human CaBP5

The 3′-end of human CaBP5 was cycled 94°C for 30 s, 55°C for 30 s, and 68°C for 2 min with primers K36 (5′-CTG AAA AGC AGC GGG AGA GAC CA) and λgt10S (5′-AGC AAG TTC AGC CTG GTA AG). The 5′-end of human CaBP5 was amplified with primers K37 (5′-CCC ATC GTT CTC ATG AGA TTG CC) and T7L (5′-GCT CTA ATA CGA CTC ACT ATA GGG) through 94°C for 30 s, 60°C for 30 s and 68°C for 2 min.

### 2.15. Cloning of mouse CaBP5

The 5′-end of mouse CaBP5 was cloned by PCR with primers K30 (5′-CTC CCC ATC TCC ATT GGC A) and T7L (5′-GCT CTA ATA CGA CTC ACT ATA GGG) through 35 cycles at 94°C for 30 s,

60°C for 30 s, and 68°C for 2.5 min. Primers K27 (5′-GCC AGC AAA TCC GAA TGA ACC TTG) and SP6L (5′-GTG AAT TGA ATT TAG GTG ACA CTA TAG) were used to amplify the 3′-end of mouse CaBP5 following the same PCR conditions.

### 2.16. Cloning of bovine CaBP5

The 5′-end of bovine CaBP5 was amplified with primers K29 (5′-CTC CCG GAC AAC CTC AGA GAT C) and T7L (5′-GCT CTA ATA CGA CTC ACT ATA GGG) at 94°C for 30 s, 55°C for 30 s and 68°C for 2 min. The 3′-end of bovine CaBP3 was cycled at 94°C for 30 s, 68°C for 2 min with primers K27 (5′-GCC AGC AAA TCC GAA TGA ACC TTG) and SP6L (5′-GTG AAT TGA ATT TAG GTG ACA CTA TAG).

### 2.17. CaBP gene structures and expression profiles

The CaBP1–5 gene structures and expression patterns were determined as previously described [1].

### 2.18. Chromosomal localization of CaBP2 and CaBP3/5 by fluorescence in situ hybridization

The localization of CaBP2 and CaBP3/5 was carried out by Hillary Heins from Genome Systems, Inc., by fluorescence in situ hybridization as described previously [1]. For example, to determine the location of the CaBP3/5 gene, DNA from clone F848 was labeled with digoxigenin dUTP by nick translation. Labeled probes were combined with sheared human DNA and hybridized to normal metaphase chromosomes derived from PHA-stimulated peripheral blood lymphocytes from a male donor in a solution containing 50% formamide, 10% dextran sulfate, and 2×SSC. Specific hybridization signals were detected by incubating the hybridized slides in fluoresceinated anti-digoxigenin antibodies followed by counterstaining with DAPI. The initial experiment resulted in specific labeling of the distal long arm of a group F chromosome. A second set of experiments was conducted in which a genomic clone from the *E2A* locus (19p13.3) was co-hybridized with clone F848. This experiment resulted in the specific labeling of the short and long arms of chromosome 19. Measurements of 10 specific hybridized chromosomes 19 demonstrated that F848 is located at chromosome 19q13.3. A total of 80 metaphase cells were analyzed for each clone with 75 exhibiting specific labeling.

### 2.19. Expression of CaBPs in Escherichia coli

The coding sequence for the long and short human CaBP1 was amplified from human retina cDNA library as described above under cloning of short human CaBP1. The coding sequence for the bovine CaBP1 was amplified from bovine retina cDNA library with primers K53 (5′-CAT ATG GGA AAC TGT GCC AAG CGG CC) which placed an *Nde*I site on the ATG and K8 (5′-TCA GTG ATG GTG ATG GTG ATG GCG GGA CAT CAT CCG GAC AAA C) which added a $His_6$-tag at the C-terminus of the protein. The PCRs were cycled 35 times at 94°C for 30 s, 56°C for 30 s, 68°C for 2 min. The coding sequence for mouse CaBP5 was amplified from mouse retina cDNA library with primers K42 (5′-CAT ATG CAG TTT CCA ATG GGT CCT G) and either K16 (5′-TCA GCG AGA CAT CAT CTT CAC AAA C) or K17 (5′-TCA GTG ATG GTG ATG GTG ATG GCG AGA CAT CAT CTT CAC AAA CTC) which added a $His_6$-tag at the C-terminus of the protein. The reactions were cycled 35 times through 94°C for 30 s, 60°C for 30 s, and 68°C for 1.5 min. The short form of mouse CaBP5 was amplified with primers K60 (5′-CAT ATG GGT CCT GCC TGC ATC TTC) and K16 (5′-TCA GCG AGA CAT CAT CTT CAC AAA C) at 94°C for 30 s, 60°C for 30 s and 68°C for 1.5 min. The PCR product for each CaBP was cloned in pCRII-TOPO vector and sequenced by dyedeoxyterminator sequencing (ABI-Prism, Perkin-Elmer). The coding sequences were cloned as fragments *Nde*I–*Bam*HI in pET-3b vector (Novagen). CaBPs were expressed in BL21 bacteria after induction with 0.2 mM IPTG.

### 2.20. Expression of CaM

The coding sequence for sea urchin CaM was amplified by PCR with primers K30 (5′-CAT ATG GCT GAC CAA CTC AC) and K24 (5′-TCA GTG ATG GTG ATG GTG ATG CTT AGC CGT CAT CAT TTG CAC A), which inserted a

*Nde*I restriction site on the ATG and a $His_6$-tag at the C-terminus of the protein. The reactions were cycled 35 times through 94°C for 30 s, 54°C for 30 s, 68°C for 1 min and the PCR product was cloned in pCRII-TOPO vector and sequenced by dyedeoxyterminator sequencing (ABI-Prism, Perkin-Elmer). The coding sequence was then transferred as a fragment *Nde*I–*Bam*HI in pET-3b vector (Novagen). CaM was expressed in BL21 bacteria after induction with 0.2 mM IPTG and purified on $Ni^{2+}$-NTA column.

### 2.21. Purification of recombinant calcineurin

All purification steps were carried out at 4°C. Calcineurin was over-expressed in *E. coli* [35] and the construct has been obtained from Dr. Jun O. Liu. Bacteria cell pellet was ultrasonicated in 10 mM BTP, pH 7.5, containing protease inhibitors, centrifuged and supernatant was loaded on $Ni^{2+}$-NTA resin. Column was washed with 50 mM $NaH_2PO_4$, pH 8.0, containing 300 mM NaCl and $His_6$-tagged calcineurin was eluted by 250 mM imidazole in 50 mM $NaH_2PO_4$, pH 8.0 with 300 mM NaCl. Fractions with the highest amount of calcineurin were pooled, dialyzed against 10 mM BTP, pH 7.5, containing 3 mM $CaCl_2$ and loaded on an equilibrated CaM-Sepharose column. The resin was washed with 10 mM BTP, pH 7.5, and 500 mM NaCl. Proteins were eluted with 10 mM BTP, pH 7.5, containing 5 mM EDTA. After analysis of purity of proteins on 12% SDS–PAGE, fractions containing the recombinant calcineurin were pooled, dialyzed and stored at −20°C before used for future experiments.

### 2.22. Direct assay for $Ca^{2+}$-binding

$Ca^{2+}$-binding parameters were obtained by the equilibrium dialysis method using an Equilibrium Dialyzer (Amica, Columbia, MD, USA). The apparatus consisted of two fluid-containing chambers (protein and buffer chambers) separated by a thin dialysis membrane (molecular mass cutoff, 5 kDa). The protein chamber contained 200 μl of 0.27 μg/μl GCAP2, 0.45 μg/μl GCAP1 or 0.09 μg/μl GCAP1(P50L) in 10 mM BTP, pH 7.5, with 150 mM NaCl plus addition of $^{45}Ca^{2+}$ (1 μCi). The buffer chamber contained 200 μl of this same buffer excluding any proteins and $^{45}Ca^{2+}$ plus the addition of a known amount of cold $Ca^{2+}$. The fluid in the two chambers was allowed with rotation to come to equilibrium after 12 h at 25°C. Fifteen different dialysis experiments were performed at various cold $Ca^{2+}$ concentrations (0, 0.1, 0.3, 1, 3, 9, 30, 90, 150, 300 μM).

### 2.23. Preparation of [$^{33}P$]phosphopeptide

The synthetic peptide (DLDVPIPGRFDRRVSVAAE) (∼2 mg), corresponding to the segment of the RII subunit of cAMP-dependent kinase (cAMP-dependent protein kinase (Promega)), was radioactively labeled by $^{33}P$ on the serine residue, using catalytic subunit of cAMP-dependent protein kinase (2500 U) and 6 mM ATP with [γ-$^{33}P$]ATP (107 700 cpm/nmol) as a substrate. Reaction was carried out for 2 h at 30°C, in 10 mM BTP, pH 7.5, with 10 mM $MgCl_2$ (total volume 1 ml). The time course of phosphorylation was followed by filter paper technique using P-cellulose paper in 75 mM $H_3PO_4$ to wash out the excess of [γ-$^{33}P$]ATP from the phosphorylated peptide [36].

### 2.24. Purification of [$^{33}P$]phosphopeptide

First, peptide mixtures were purified on $Ga^{3+}$-immobilized affinity metal ion chromatography (IMAC) to separate phosphorylated/unphosphorylated peptides [37]. After equilibration with 0.1% $CH_3COOH$ of $GaCl_3$ (Alfa Aesar, #35698) charged chelating Sepharose gel (Pharmacia, #17-0575-01), peptides were loaded on the resin. Unbound peptides were removed by exhaustive wash with 0.1% $CH_3COOH$ and $^{33}P$-labeled phosphopeptides were eluted with 1 M $NH_4OH$. Next, the $Ga^{3+}$ IMAC-purified phosphopeptides were injected onto a $C_{18}$ high performance liquid chromatography column (4.6×150 mm, Hewlett Packard XDB-$C_{18}$). Peptides were eluted employing a linear gradient from 0% to 50% $CH_3CN$ with 0.05% TFA during 30 min at a flow rate of 1 ml/min. The absorbance at 220 nm was monitored, and a small aliquot (2 μl) from each fraction was used for counting of $^{33}P$ activity. Fractions with the highest activity were dried down using a SpeedVac.

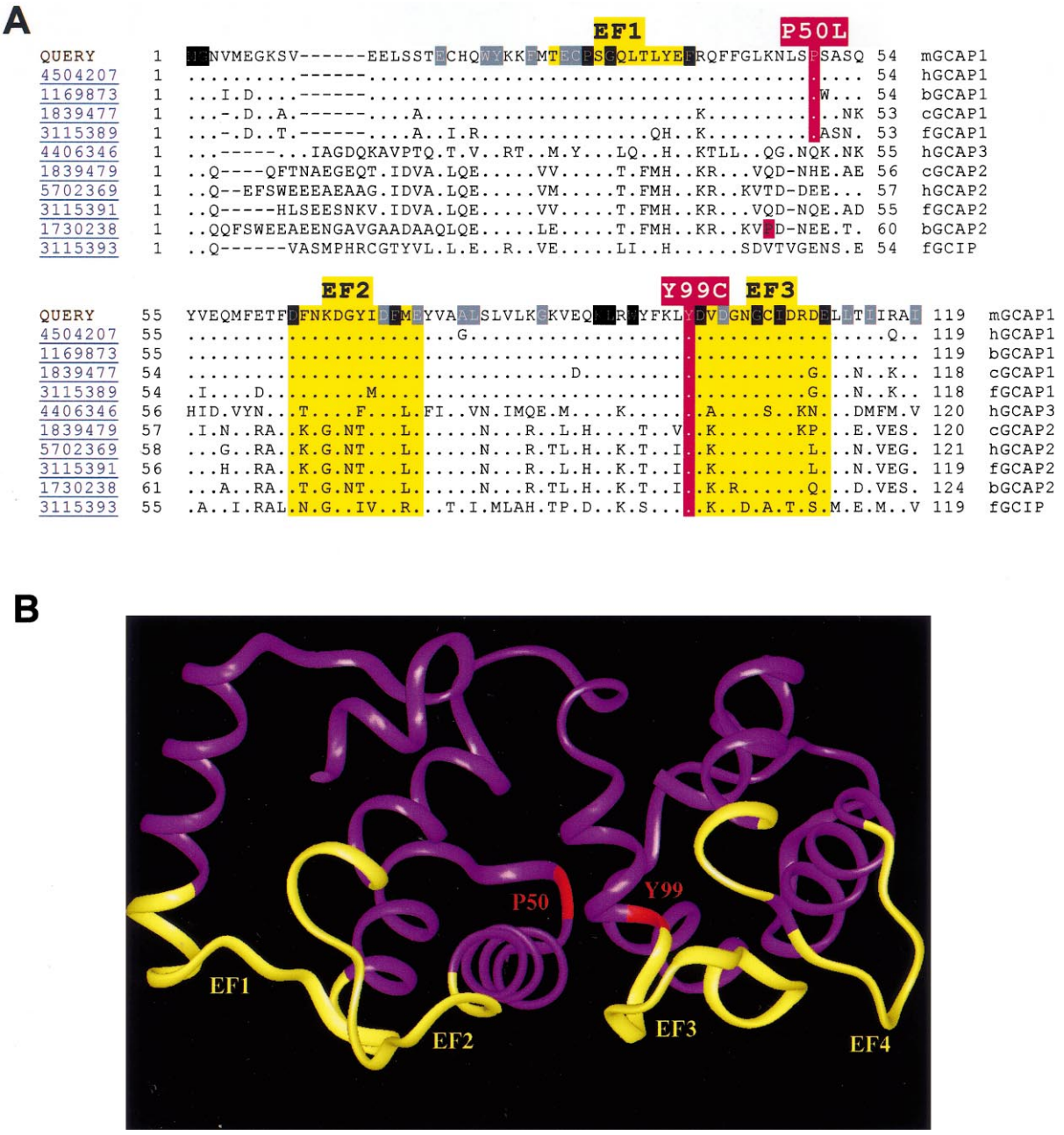


Fig. 2. P50L and Y99C mutations in GCAP1. A: Sequence alignment of the N-terminal portion of GCAPs and frog GCIP. Y99C is conserved in all GCAPs. P50L is conserved only in GCAP1 from various species. Numbers in the query column refer to links to the GenBank. The query sequence was mouse GCAP1 (mGCAP1). B: Three-dimensional model of GCAP1 indicating the location of P50L and Y99C. The model was generated as described in Section 2.

### 2.25. Phosphatase assay

Stimulation of calcineurin (0.05 μg) by CaBPs was determined by dephosphorylation of phosphopeptide (100 000 cpm/nmol) in 50 μl reaction volumes. Dephosphorylation was performed in the presence of 20 mM Tris, pH 8.0, 100 mM NaCl, 6 mM $MgCl_2$, 0.5 mM dithiothreitol, 0.1 mM $CaCl_2$ and calcineurin stimulators (CaM or CaBPs) for 20 min at 30°C. The reactions were terminated by addition of 30 μl

acetic acid and the released $^{33}P$ was washed out from the peptide using P-cellulose paper in 75 mM $H_3PO_4$. Data were expressed as the number of pmol of released $^{33}P$ in 1 min.

### 2.26. Models of CaBPs

Homology models of human CaBP1, bovine CaBP2 and human CaBP5 were created on the basis of the crystal structure of human CaM in its $Ca^{2+}$-bound state (PDB entry: 1CLL at 1.75 Å resolution [38]), making use of the sequence alignment between these proteins [14]. Because the N-terminal end of CaM is significantly shorter than the N-terminus of the human CaBPs, residues 1–19 of human CaBP1 and residues 1–22 of human CaBP5 were omitted from the model. The models were generated with the HOMOLOGY module of the INSIGHT II software (Molecular Simulations, Inc., San Diego, CA, USA) using established homology modeling protocols [39]. In short, protein backbone coordinates were taken from CaM for all helices, strands, EF hands and loops with identical lengths. Coordinates of conserved side chains were kept. Non-conserved side chains were built from a rotamer database. The four residues insertion in the long central helix of the CaBPs between the two domains of the proteins was assumed not to distort or cause significant bending of this structural element. Therefore, the residues were built in helical conformation. Experimental support for this approach comes from a mutation study with CaM in which two residues were deleted from the central helix. A crystal structure showed only helix shortening leading to a different separation of the two protein domains and a change in relative orientation of the domains [40]. Coordinates for the loop with the one residue insertion were obtained by transplantation from an appropriate PDB entry. Finally, 2000 steps of conjugate gradient energy minimization were executed to alleviate small irregularities in the structure.

### 2.27. Homology model of GCAP1

GCAP models were created on the basis of the crystal structure of unmyristoylated recoverin (PDB entry: 1REC [41]), making use of the alignment from [14,15]. The model was created with the HOMOLOGY module of the INSIGHT II software (Molecular Simulations, Inc., San Diego, CA, USA) using established homology modeling protocols [39]. In short, protein backbone coordinates were borrowed from recovering for all helices, strands, EF hand motifs, and loops with identical lengths. The coordinates for other loops were transplanted from appropriate PDB entries. Coordinates of conserved side chains were kept. Non-conserved side chains were built from a rotamer database. Finally, 2000 steps of conjugate energy minimization were executed to alleviate small irregularities in the structure.

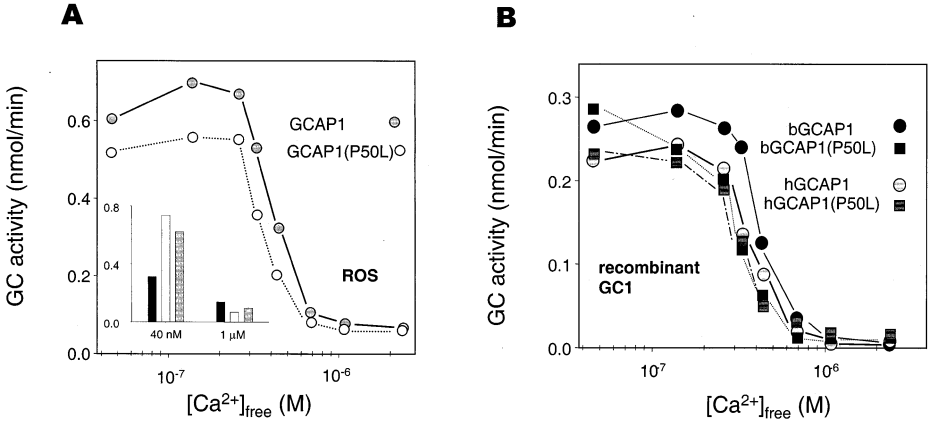


Fig. 3. GC stimulation by GCAP1 and recombinant GCAP1 mutants as a function of free $Ca^{2+}$. A: $Ca^{2+}$ titration of GC activity in washed ROS membranes in the presence of 0.5 μg bGCAP1, and 0.5 μg hGCAP1P50L. Inset, the activity of ROS-GC in 40 nM and 1 μM $Ca^{2+}$ without GCAP (black), with bGCAP1 (white) and with hGCAP1P50L (gray). B: $Ca^{2+}$ titration of recombinant bGC1 activity in presence of GCAPs (0.5 μg).

## 3. Results

### 3.1. Biochemical properties of GCAP1(P50L)

Compared with native GCAP1, the previously described GCAP1(Y99C) mutant [31] showed a characteristic change in $Ca^{2+}$ sensitivity as a gain of function [31,42]. The mutated residue Y99, flanking the EF3 hand (Fig. 2A,B), is highly conserved among GCAPs and other CaBPs. Its replacement by Cys lowers the affinity for $Ca^{2+}$-binding to the EF3 loop [31,42]. Another mutation, P50L, was identified recently and suggested to be associated also with autosomal cone dystrophy [59]. P50, in contrast to Y99, is located in a relatively variable region between EF1 and EF2, and only conserved among GCAP1s of various species (Fig. 2A). To investigate whether the replacement of P50 by L changes the biochemical properties of the mutant GCAP1, we tested the recombinant bovine and human GCAP1(P50L) mutants for their ability to stimulate GC as a function of $Ca^{2+}$. For most assays, we used native bovine ROS as sources of GC activity [43]. However, because ROS preparations most likely contain a mixture of GC isoforms, we used also recombinant bovine and human GC1 expressed in HEK293 cells. We found that GCAP1(P50L), similarly to GCAP1, activates photoreceptor GC at $[Ca^{2+}] < 100$ nM and inhibits it at micromolar concentrations (Fig. 3A, inset). GCAP1(P50L) and GCAP1 are identical in stimulation of ROS-GC in a range of free $[Ca^{2+}]$ from 4 nM to 2 μM (Fig. 3A). $Ca^{2+}$ dependencies of recombinant GC1 stimulation by GCAP1 and P50L mutants were comparable to those obtained for ROS-GC (Fig. 3B). In addition, human and bovine GCAP1(P50L) activated photoreceptor GC to

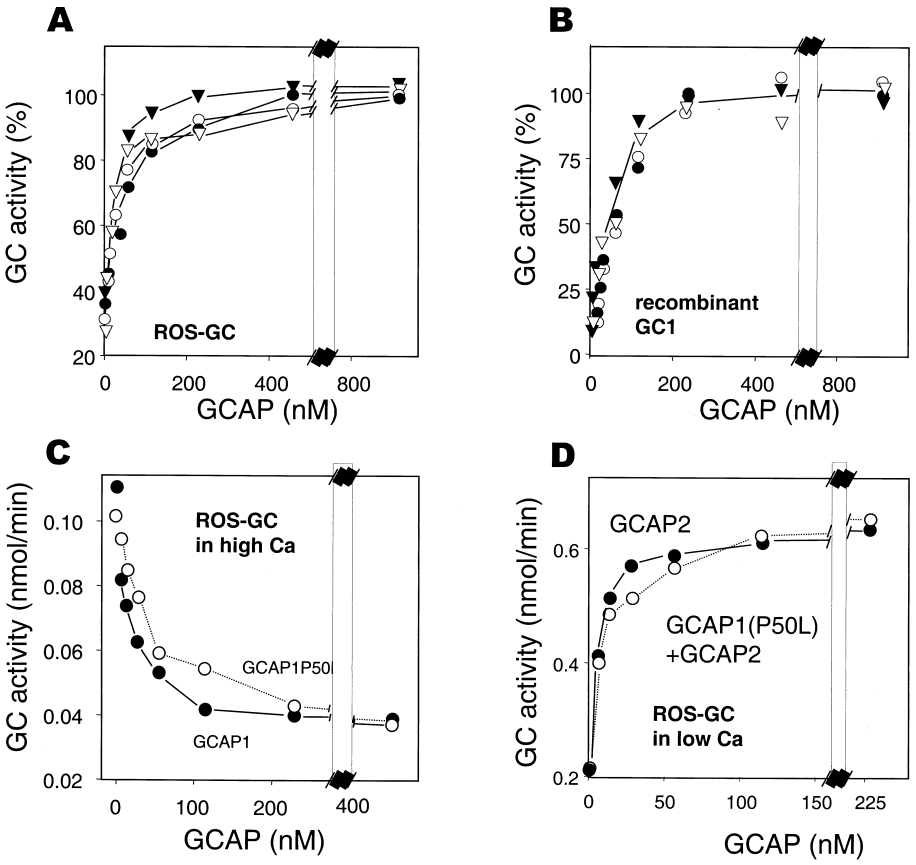


Fig. 4. Reconstitution of GC activity (A) in ROS membranes and (B) recombinant bGC1. A and B: Reconstitution of GC with 0.5 μg bGCAP1 ●, hGCAP1 ○, bGCAP1P50L ▼ and hGCAP1P50L ▽ as % of maximum stimulation. C: Competition in high $Ca^{2+}$ between indicated concentrations of bGCAP1 and 0.5 μg of bGCAP1(P50L). D: Dose-dependent stimulation of ROS-GC by GCAP2 and mixture of GCAP2 with GCAP1(P50L).

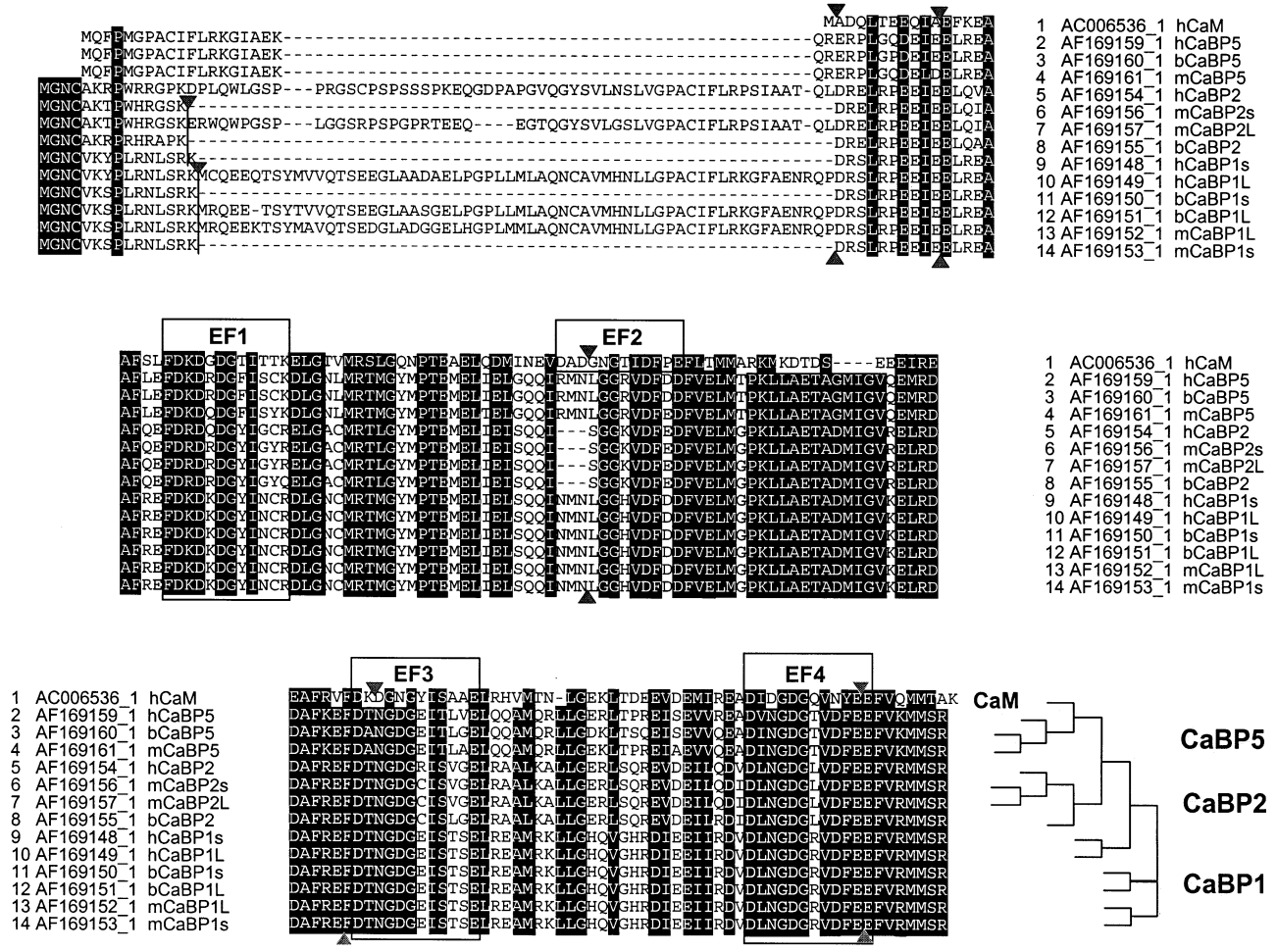


Fig. 5. Alignment of the deduced amino acid sequences of human (h), bovine (b), mouse (m) CaBPs with hCaM. The numbers in the column identifying the polypeptides refer to GenBank accession numbers. Identical residues or conservative substitutions in at least 13 of 14 sequences are shown in white letters on black background. The conservative substitutions are Q = E = D = N; S = T = A; V = M = I = L; K = R; Y = W = F. Arrow heads indicate intron–exon junctions for the human CaBP1 gene (presumably conserved in other mammalian genes). L and S indicate the long or short spliced forms of CaBPs. Note that EF2 is present only in CaM.

the same relative extent as native GCAP1. Both stimulate GC activity in a dose-dependent fashion with half-maximal activation occurring at ~100 nM and saturation at ~200 nM (Fig. 4A,B). These results indicate that $Ca^{2+}$-dependent stimulation of GC by GCAP1(P50L) and GCAP1 are indistinguishable.

In addition to stimulation of GC by $Ca^{2+}$-free GCAP, we also tested inhibition of basal GC activity by $Ca^{2+}$-bound GCAPs [43]. GC activity is unaffected by up to 2 μM $[Ca^{2+}]_{free}$, but is ~50% inhibited by the $Ca^{2+}$-loaded form of GCAP1. GCAP1(P50L) inhibition of basal activity is nearly identical (Fig. 4C), and dose dependence is comparable with that of activation. These data suggest that GCAP1(P50L) inhibits photoreceptor GC with these same enzymatic properties as native GCAP1. We further tested cooperativity of GC stimulation in the presence of GCAP2, but did not observe any changes in GC activity regulation in its presence (Fig. 4D).

### 3.2. Distinct properties of GCAP1(P50L)

To further investigate the influence of the P50L mutation on biochemical properties of GCAP1, we measured $Ca^{2+}$-binding parameters by equilibrium dialysis. Ten μM mutant GCAP1 (or control GCAPs) was incubated with 0–300 μM $^{45}Ca^{2+}$ in a

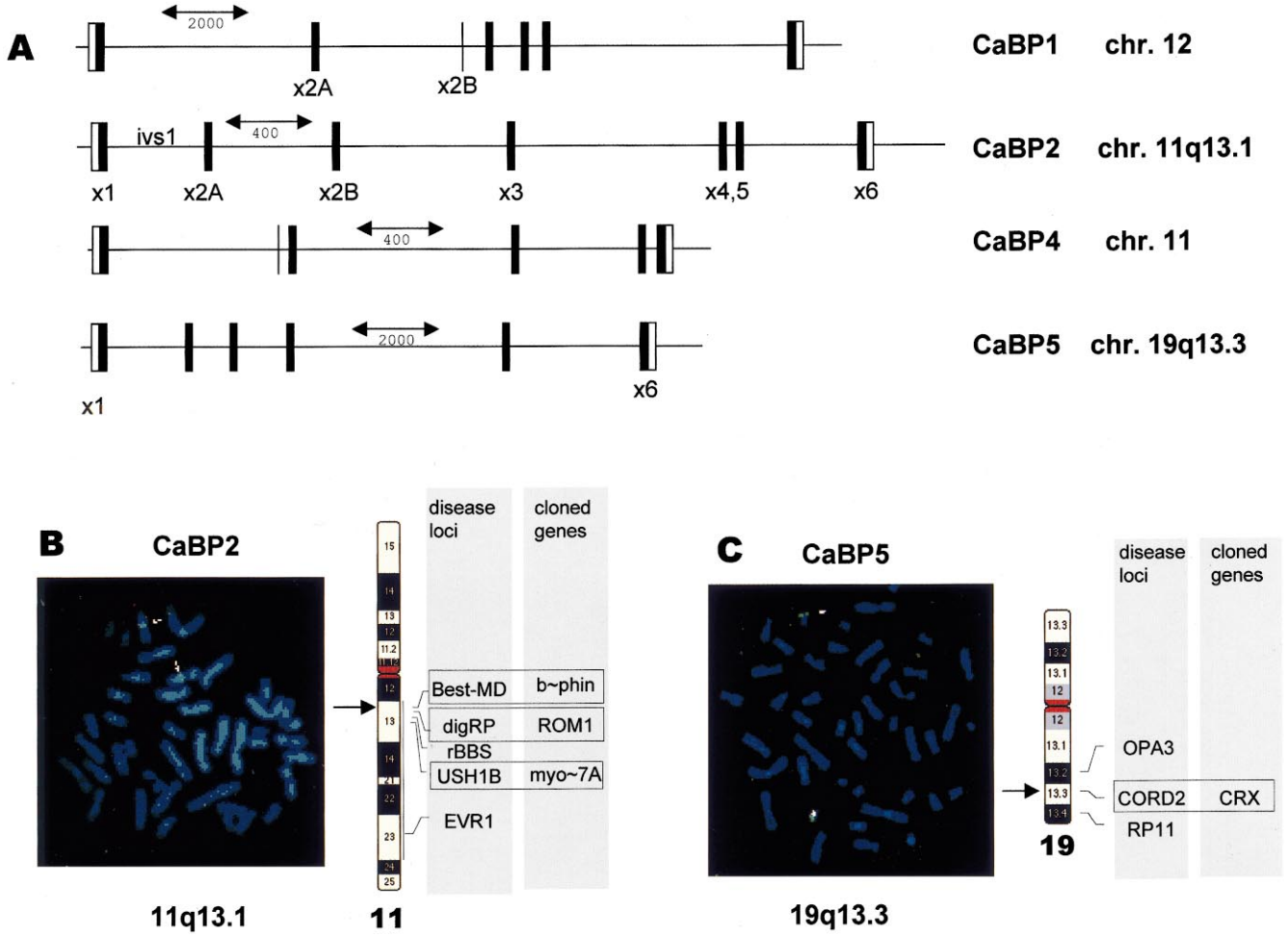


Fig. 6. Chromosomal localization and organization of human CaBP genes. A: Gene structures of CaBP1,2 and CaBP4,5. The coding regions of the CaBP2 gene are shown as black boxes, non-coding regions of exon 1 and exon 6 are shown as white boxes. Introns are shown as lines. The scales are in base pairs. FISH of CaBP2 (B) and CaBP5 (C) gene probes to human metaphase chromosomes. The arrow indicates specific labeling on chromosome 11q13.1 and 19q13.3 for CaBP2 and CaBP5, respectively. The respective chromosomes are depicted on the right. Disease loci identified near the CaBP loci are indicated (for details and references, see http://www.sph.uth.tmc.edu/RetNet/disease.htm. Boxes indicate correlation of a gene locus to a cloned gene (b~phin, bestrophin; ROM1, rod membrane protein 1; myo~7A, unconventional myosin 7A; CRX, cone-rod homeobox gene).

dialysis chamber, and the uptake of calcium measured after 24 h of equilibration. The results show that the apparent dissociation constants for $Ca^{2+}$-binding in normal and mutant GCAPs are nearly identical (5.2 and 5.6 μM for GCAP1 and GCAP1(P50L), respectively), while the number of $Ca^{2+}$-binding sites in mutant GCAP1 is significantly reduced (2.9 sites for GCAP1 vs. 1.4 sites for GCAP1(P50L)). Approximately 3 mol of $Ca^{2+}$ bound to GCAP1 is consistent with the presence of three functional EF hands in the native polypeptide (Fig. 1B). Reduction to less than two sites in GCAP1(P50L) indicates most likely impaired $Ca^{2+}$-binding in EF2, the site nearest to the P50L mutation. In other mutants disabling $Ca^{2+}$-binding to the EF2 loop, EF2 was shown to be unimportant for $Ca^{2+}$-dependent stimulation of GC [33], consistent with a lack of distinction in $Ca^{2+}$-dependent GC stimulation by the mutant GCAP1 (Fig. 3B). Inability to bind free $Ca^{2+}$ could lead to changes in cone photoreceptor $Ca^{2+}$ homeostasis and thus trigger a slow cone degeneration.

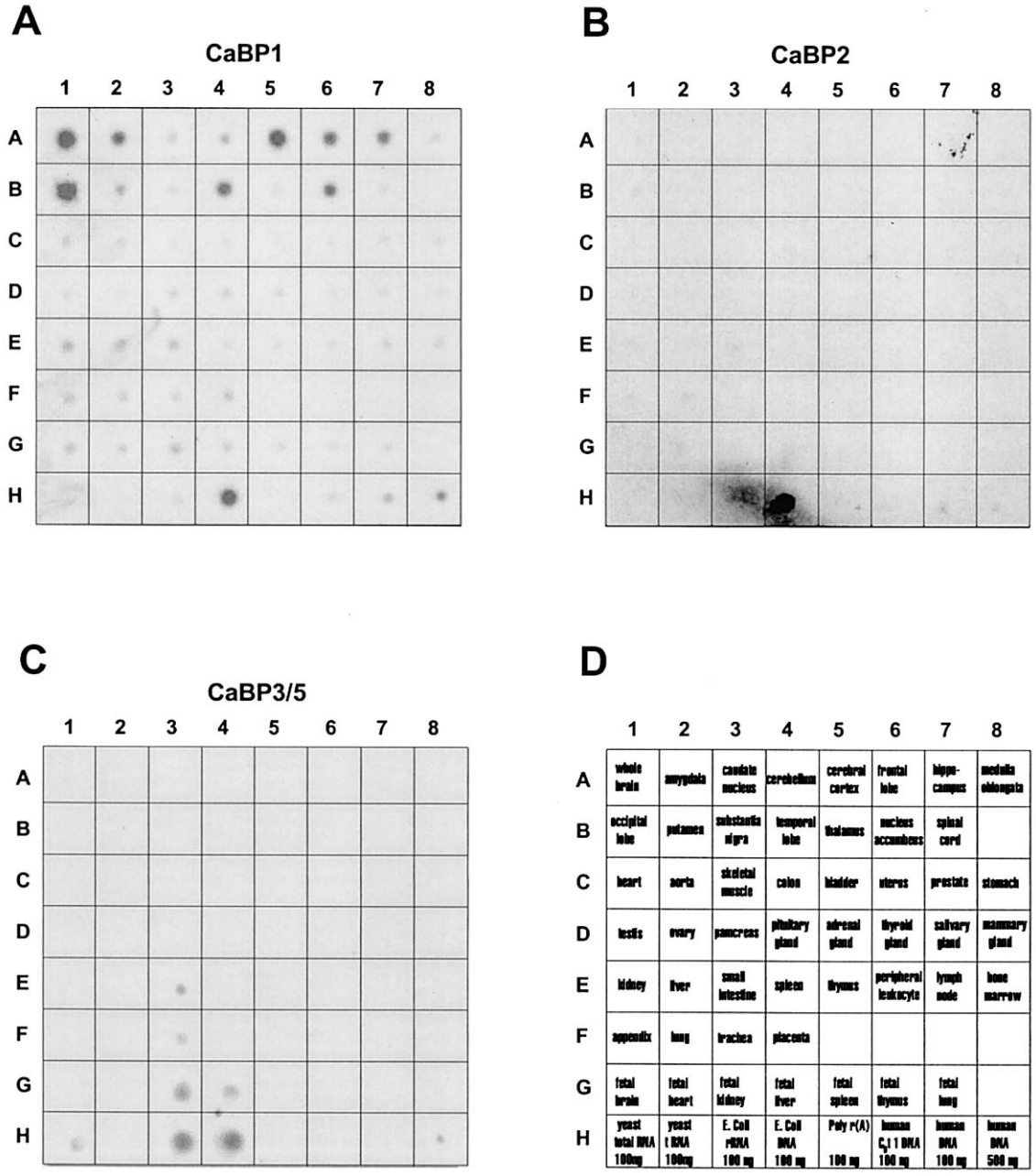


Fig. 7. Tissue distribution of CaBP mRNAs by dot blot analysis. RNA dot blot containing normalized amounts of 89–514 ng of poly(A)$^+$ RNA from various human tissues was probed with a $^{32}$P-labeled human CaBP1 cDNA (A), human CaBP2 (B) or human CaBP3 (C) cDNA. D shows the tissue origin of poly A$^+$ RNA from the master blot.

### 3.3. Novel subfamily of CaBPs

Five novel neuron-specific CaBPs, CaBP1–CaBP5, were recently cloned 'in silico' and subsequently from retinal libraries [1]. These proteins display a new combination of functional/non-functional EF hand motifs and presence/absence of N-terminal myristoylation. Amino acid alignment and dendrogram of CaM-like CaBPs (Fig. 5) showed that the major divergence of CaBPs from the common ancestor, likely a CaM-like protein with four EF domains, is the inactivation of the second $Ca^{2+}$-binding loop. Inactivation is accomplished by mutations and deletions of residues important for $Ca^{2+}$ coordination, or

alternative splicing. In addition to EF2 inactivation, CaBP1 contains a consensus sequence for myristoylation not present in CaM. A large portion of the CaBP1 sequence is identical to previously published caldendrin [27] and calbrain [44]. We assume that caldendrin contains additional sequence at the N-terminus that resulted from alternative splicing, while calbrain represents a truncated sequence of CaBP1. Retina-specific CaBP2 appears to be a minor component in the retina, also is presumably myristoylated and has a 3-amino acid deletion in the EF2 loop rendering it non-functional for $Ca^{2+}$-binding. In contrast to CaBP1 and CaBP2, the N-terminus of CaBP5 carries no consensus sequence for myristoylation (Fig. 5). The N-terminal exon of the CaBP4 gene has not been unambiguously identified [1].

### 3.4. *CaBP5/CaBP2 gene structures and chromosomal localization*

CaBPs have gene structures almost identical to CaM, with only one intron (ivs3) positioned slightly differently (Fig. 5). The genes encoding CaBP2 and CaBP4 are the smallest among CaBPs encompassing only about 3 kb genomic sequence (Fig. 6A). Well-conserved CaBP and CaM gene structures suggest that the CaBPs evolved from a CaM-like ancestral gene. Fluorescent in situ hybridization (FISH) to human metaphase chromosomes located the CaBP2 gene to chromosome 11q13.1 (Fig. 6B), while a CaBP5 probe located this gene on chromosome 19q13.3 (Fig. 6C, [1]). The 11q13.1 locus is very close to those of Best's macular dystrophy and Usher syndrome 1B for whom the causative genes are known, and recessive Bardet–Biedl syndrome for which the gene is still unidentified. Moreover, the 19q13.3 locus, near a cone/rod dystrophy locus (CORD2) linked to a transcription factor gene (CRX), is close to RP11 and Opa3 involving retinal atrophies for which the causative genes are unknown (Fig. 6C). In contrast to S100 CaBPs and the GCAP1/2 gene array, CaBP genes do not appear clustered on the same chromosome (the CaBP4 and CaBP2 genes, both on chromosome 11, are at least 40 kb apart and not clustered). The nearly identical gene structures of CaBPs, however, indicate evolutionary rela-

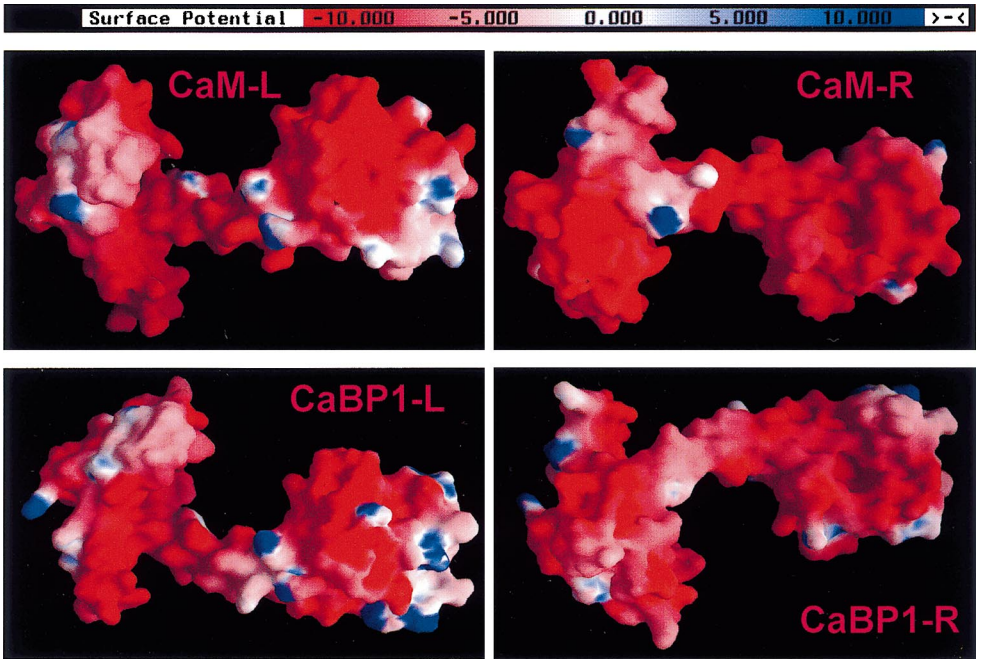


Fig. 8. Three-dimensional model of CaM and CaBP1. Color-coded molecular surface of CaM and CaBP1 according to electrostatic potential. Panels L and R are rotated 180° around the horizontal axis. The panels show that the third and fourth EF hand motifs contribute to the strongly negative potential on both sides of the molecule. The scale bar above each picture shows the color scheme: units are in kT/e. Figures were generated as described in Section 2 [61].

tionship with a common ancestor by gene duplication events and translocation to different chromosomes.

### 3.5. Tissue distribution of CaBPs other than retina

Master RNA blots containing poly(A)$^+$ RNA from 50 human tissues hybridized with CaBP1 as a probe showed presence of CaBP1 in whole brain (A1), occipital lobe (B1) and cerebral cortex (A5). A weak hybridization signal just above background (negative control, *E. coli* DNA, H4) was observed in the frontal lobe (A6), hippocampus (A7), temporal lobe (B4) and nucleus accumbeus (B6) (Fig. 7A). CaBP1 reverse transcription (RT)-PCR products were observed in retina and cerebellum (data not shown). Hybridization of the master RNA blots with the CaBP2 probe is shown in Fig. 7B. No signal was detected above the background (negative controls H3 and H4). In contrast to CaBP1, CaBP2 and CaBP5 are specifically expressed in the retina (Fig. 7C). Furthermore, RT-PCR was performed on total RNA isolated from diverse mouse tissue and CaBP2 and CaBP5 products were seen only in retina. As a control, GPDH was amplified in every tissue. The CaBP mRNA tissue distribution analyzed by different methods consistently shows specific expression of CaBP2 and CaBP5 in retina. CaBP1 mRNAs are present in retina and also in brain, while it is a minor transcript in the eye and not observed elsewhere. The CaBP4 expression pattern was not determined using this master blot.

### 3.6. Structural predictions

By computer modeling, we compared the CaBP structures with those of other CaBPs of known tertiary structure. The four residue insertion in the long central helix of the CaBPs between the two domains of the proteins was assumed not to distort or cause significant bending of this structural element (Fig. 8). Therefore, the residues were built in helical conformation. Experimental support for this approach comes from a mutation study with CaM in which two residues were deleted from the central helix. A crystal structure showed only helix shortening leading to a different separation of the two protein domains and a change in relative orientation of the domains [40]. Coordinates for the loop with the one residue insertion were obtained by transplantation from an appropriate PDB entry. Finally, 2000 steps of conjugate gradient energy minimization were executed to alleviate small irregularities in the structure. These modeling data suggest that CaBPs may have an overall structure very similar to CaM (Fig. 8).

### 3.7. In search for function for CaBPs

CaM and CaM-like proteins are multifunctional and stimulate or inhibit a variety of targets. Several candidate targets for CaBPs were tested recently [1]. We have established that CaBPs can substitute for CaM in inhibition of G-protein-coupled receptor kinases, and stimulation of CaM kinase II. Further-

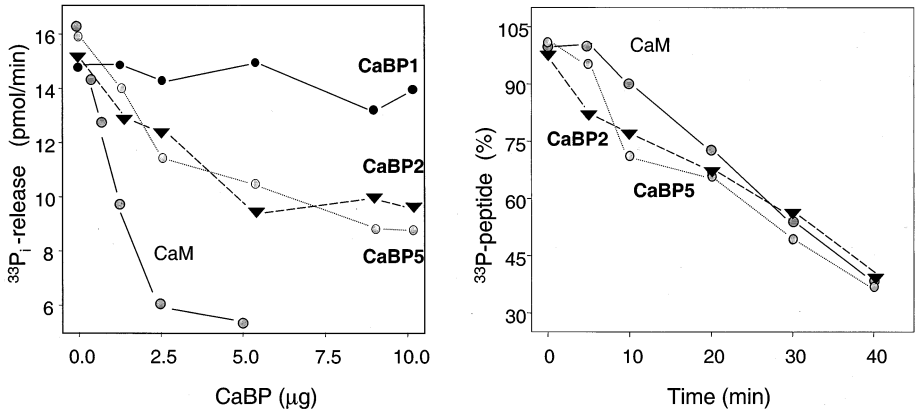


Fig. 9. Dephosphorylation of phosphopeptide by calcineurin in the presence of CaM and CaBPs. Dose-dependent and time course for CaBPs- and CaM-mediated dephosphorylation by calcineurin as a % of $^{33}$P radioactivity at time zero. Assays were performed as described under Section 2 and shown data are representative of two separated experiments.

more, it has been shown that CaBP1 binds avidly to cytoskeletal proteins [27]. Here, we tested effects on CaBPs of another enzyme that is stimulated by CaM, protein phosphatase B-calcineurin [45,46]. A candidate approach was also used in a search for possible effector protein of other CaBPs. Because of potent activation of calcineurin by CaM and significant homology of CaBPs with CaM, we tested CaBPs in stimulation of phosphatase activity of calcineurin. A phosphorylated peptide derived from cAMP-dependent protein kinase catalytic subunit [47] served as a substrate in the calcineurin activity [48]. Peptide dephosphorylation by calcineurin was increased in presence of CaM, CaBP2 and CaBP5, and was linear for up to 40 min (Fig. 9A). However, peptide dephosphorylation was less effective in the presence of CaBP2 and CaBP5 as compared to CaM, and required higher concentration of CaBPs (Fig. 9B). CaBP1 had no significant effect on calcineurin activity.

Together, these results suggest that CaBP can substitute for CaM in various assays. However, there is a clear distinction and specificity between different CaBPs. Thus, some cellular regulations previously assigned to CaM may be carried out in vivo by CaBPs. On the other hand, the in vitro assays are prone to error, due to dilution of interaction partners, or erroneous choice of the interaction partners that will not co-localize in vivo. These results must be further evaluated in independent assays in the future, including genetic methods.

## 4. Discussion

$Ca^{2+}$ ions play an important role in the physiology of all eukaryotes. Over many years, the vertebrate retina has been a model tissue that has been used to decipher principles of these regulatory processes. In particular, $Ca^{2+}$ modulation of phototransduction events received ample attention, while other regulatory mechanisms of the visual system are less well understood. In the photoreceptor cell, light causes bleaching and activation of photoreceptor molecules, which in turn activate a cascade of enzymatic reactions that culminates in cGMP and $Ca^{2+}$ concentration decreases. In contrast to most neurons, the decrease, and not increase, in free $Ca^{2+}$ concentration is the signal that activates enzymes and proteins of phototransduction. The most critical event in return to the dark state is activation of GCs by $Ca^{2+}$-free GCAPs that leads to restoration of high levels of cGMP, depleted by the activation of phototransduction cascade [7].

### 4.1. The GC/GCAP modulatory system

Two membrane-associated GCs, GC1 and GC2, were identified in the mammalian retina [49–51], regulated by at least three GCAPs (GCAP1–3) [1,14–16,52]. The multi-domain structure of membrane GCs implies a complex, multi-ligand target that has only been partially explored. The single subunit GC consists of an extracellular receptor-like binding domain, a transmembrane segment, a kinase-like domain, a dimerization motif, and a catalytic domain. GCAPs interact with GC through the intracellular domain [53,54], modulating GC activity. GCAPs have nearly identical function, but the sequence similarity of GCAP3 with GCAP1 and GCAP2 is only 57% and 49%, respectively. Recombinant GCAP3 and GCAP2 stimulate GC1 and GC2 in low $[Ca^{2+}]_{free}$ and inhibit GCs when $[Ca^{2+}]_{free}$ is elevated, unlike GCAP1 which only stimulates GC1. The intron/exon arrangement of the GCAP3 gene is identical to that of the other two GCAP genes. However, while the GCAP1 and GCAP2 genes are arranged in a tail-to-tail array on chromosome 6p in human [55], the GCAP3 gene is located on 3q13.1, suggesting an ancestral gene duplication/translocation event [52].

Although the tertiary structures of CaBPs containing multiple EF hand motifs appear remarkably conserved, their amino acid sequences are quite divergent. Proteins from the CaM superfamily contain four EF hand motifs, some of which are non-functional due to insertions that alter the spatial arrangements and prevent interaction with $Ca^{2+}$. In each structure, the four EF hands form two domains: EF1 and EF2 interact with one another to form the amino-terminal domain, and EF3 and EF4 form the C-terminal half of the molecule. The backbone structure of $Ca^{2+}$-bound GCAP2 is very similar to that of recoverin and neurocalcin [56], and contains a short U-shaped inter-domain linker that positions the two domains in close contact with one

another forming a bi-lobed, globular shape with pseudo C2 symmetry. Three $Ca^{2+}$ ions are bound to EF2, EF3 and EF4 of GCAPs, but not to EF1 because the binding loop is distorted from a favorable $Ca^{2+}$-binding geometry by C35 and P36 at the third and fourth positions of the 12 residue loop, preventing coordination of $Ca^{2+}$. The precise structure of the physiologically active $Ca^{2+}$-free GCAPs is presently unknown.

Only GCAPs have been shown to activate photoreceptor GC in their $Ca^{2+}$-free forms, consistent with their role in phototransduction [6]. In biochemical assays, two other GC activators, S100β (also termed GD-GCAP [57]) and neurocalcin [58], have recently been shown to activate GC1 in the $Ca^{2+}$-occupied form in vitro. The physiological significance of their GC activation by S100 and neurocalcin is unclear.

### 4.2. Mutations in GCAP1 causing dominant cone dystrophy

Cone dystrophies are characterized by progressive loss of color vision, photophobia, and visual acuity. The occurrence is relatively frequent, the autosomal dominant form occurs in approximately one in 10 000 births. Several loci have been identified in autosomal dominant cone and cone-rod dystrophies. Those associated with identified genes include mutations in peripherin/RDS (6p12), GCAP1/2 (locus *GUCA1* on 6p21), GC1 (locus *GUCY2D* on 17p), and the transcription factor CRX (19q). A Y99C mutation in GCAP1 has recently been found to be associated with autosomal dominant cone dystrophy [31,42]. The biochemical analysis of GCAP1(Y99) suggested constitutive activation of GC that was not properly inactivated by dark levels of $Ca^{2+}$, perturbing homeostasis of $Ca^{2+}$ in photoreceptor cells in the dark, ultimately leading to degeneration of these cells. As a consequence of the GCAP1(Y99) mutation, the $Ca^{2+}$ sensitivity of cones, which have high levels of GCAP1, is markedly altered, causing persistent stimulation of GC1 under physiological dark conditions [31]. These results are consistent with a model in which enhanced GC activity in dark-adapted cones leads to elevated levels of cytoplasmic cGMP.

A second GCAP1 mutation (P50L) was identified in several small British families afflicted with autosomal cone dystrophy [59]. In this study, we focused on biochemical properties of GCAP1(P50L), a mutation suspected to cause a milder form of autosomal dominant cone dystrophy. We present evidence that like GCAP1(Y99) mutant, GCAP1(P50L) has modified $Ca^{2+}$-binding properties. The P50L mutation, however, causes decrease in the maximal number of bound $Ca^{2+}$ ions from 3 to $\sim$2 per GCAP1, without changing the activity profile. Thus, changes in the biochemical properties of GCAP1(P50L) are more subtle than those observed for GCAP1(Y99), and this observation correlates well with the clinical observation that the Pro mutation causes a milder form of the autosomal dominant cone dystrophy.

Due to the location of the P50L mutation, it is predicted that the major effect will be on the adjacent EF2 domain and its ability to bind $Ca^{2+}$. The dominant character of this mutation in vivo is unclear because in all our enzymatic assays, GCAP1(P50L) appears to be similar to normal GCAP1. One interpretation is that the mutant protein interferes with uncharacterized $Ca^{2+}$-dependent processes of phototransduction ultimately leading to the photoreceptor dystrophy. Alternatively, the P50L mutation may interfere with dimerization of the native GCAP1 [60], depleting the amount of GCAP in the outer segments. Further understanding these pathologies will provide with additional insights in understanding the role of GCAPs in the physiology of photoreceptor cells.

### 4.3. CaBPs, a novel subfamily of $Ca^{2+}$-binding protein

In contrast to this biochemically well-defined regulation of phototransduction, we are only beginning to understand other $Ca^{2+}$-dependent regulatory processes in the retina. Recently, we have identified five homologues genes encoding CaBPs that are expressed in the mammalian retina. Several members of this subfamily are also present in other tissues. In contrast to GCAPs, the function/structure of this subfamily of CaM-like CaBPs is poorly understood. Computer-aided prediction of the three-dimensional structure suggests a close relatedness of CaBPs and CaM, and in many biochemical assays CaBPs can substitute for CaM, including stimulation of CaM kinase II and calcineurin. Because of the importance of calcineurin and CaM kinase II in many cells, and

ubiquitous expression of several CaBPs, the role of these proteins appears to be correlated to fundamental processes in these cells.

## 5. Note added in proof

Characterization of the GCAP1(P50L) mutants will also be published in: A cone-rod dystrophy caused by a destabilization of human GCAP1 by a proline to leucine mutation, by R.J. Newbold, E. Dery, S.E. Wilkie, C.E. Walker, N. Srinivasan, S.S. Bhattacharya, D.M. Hunt and M.J. Warren, Molecular Genetics, in press.

## Acknowledgements

We would like to thank Drs. Martin Warren and Shomi Bhattacharya for communicating the GCAP1(P50L) mutation before publication. We would also like to thank Dr. Jun O. Liu (MIT) for the expression vector for calcineurin. This research was supported by NIH Grants EY008061 (K.P.), EY08123 (W.B.), unrestricted grants by Research to Prevent Blindness, Inc., to the Departments of Ophthalmology at the University of Washington and the University of Utah, a Center Grant of the Foundation Fighting Blindness (FFB) to the University of Utah, and the E.K. Bishop Foundation. W.B. is a Ralph and Mary Tuck Professor of Ophthalmology, and a Senior Investigator of the Research to Prevent Blindness. Inc.

## References

[1] F. Haeseleer, I. Sokal, C.L. Verlinde, H. Erdjument-Bromage, P. Tempst, A.N. Pronin, J.L. Benovic, R.N. Fariss, K. Palczewski, J. Biol. Chem. 275 (2000) 1247–1260.
[2] J.W. Putney Jr., R.R. McKay, BioEssays 21 (1999) 38–46.
[3] C.W. Taylor, Biochim. Biophys. Acta 1436 (1998) 19–33.
[4] D.J. McConkey, Toxicol. Lett. 99 (1998) 157–168.
[5] F.A. Antoni, S.M. Smith, J. Simpson, R. Rosie, G. Fink, J.M. Paterson, Adv. Second Messenger Phosphoprotein Res. 32 (1998) 153–172.
[6] K. Palczewski, A.S. Polans, W. Baehr, J.B. Ames, BioEssays 22 (2000) 337–350.
[7] G.L. Fain, H.R. Matthews, M.C. Cornwall, Trends Neurosci. 19 (1996) 502–507.
[8] E.N. Pugh Jr., T.D. Lamb, Vis. Res. 30 (1990) 1923–1948.
[9] Y. Koutalos, K.W. Yau, Trends Neurosci. 19 (1996) 73–81.
[10] L. Lagnado, D. Baylor, Neuron 8 (1992) 995–1002.
[11] A. Polans, W. Baehr, K. Palczewski, Trends Neurosci. 19 (1996) 547–554.
[12] A.M. Dizhoor, S. Ray, S. Kumar, G. Niemi, M. Spencer, D. Brolley, K.A. Walsh, P.P. Philipov, J.B. Hurley, L. Stryer, Science 251 (1991) 915–918.
[13] W.A. Gorczyca, M.P. Gray-Keller, P.B. Detwiler, K. Palczewski, Proc. Natl. Acad. Sci. USA 91 (1994) 4014–4018.
[14] K. Palczewski, I. Subbaraya, W.A. Gorczyca, B.S. Helekar, C.C. Ruiz, H. Ohguro, J. Huang, X. Zhao, J.W. Crabb, R.S. Johnson, K.A. Walsh, M.P. Gray-Keller, P.B. Detwiler, W. Baehr, Neuron 13 (1994) 395–404.
[15] W.A. Gorczyca, A.S. Polans, I. Surgucheva, I. Subbaraya, W. Baehr, K. Palczewski, J. Biol. Chem. 270 (1995) 22029–22036.
[16] A.M. Dizhoor, E.V. Olshevskaya, W.J. Henzel, S.C. Wong, J.T. Stults, I. Ankoudinova, J.B. Hurley, J. Biol. Chem. 270 (1995) 25200–25206.
[17] S. Frins, W. Boenigk, F. Mueller, R. Kellner, K.-W. Koch, J. Biol. Chem. 271 (1996) 8022–8027.
[18] M. Kobayashi, K. Takamatsu, S. Saitoh, M. Miura, T. Noguchi, Biochem. Biophys. Res. Commun. 196 (1993) 1017.
[19] Y. Furuta, M.O. Kobayashi, T. Masaki, K. Takamatsu, Neurochem. Res. 24 (1999) 651–658.
[20] B.W. McFerran, J.L. Weiss, R.D. Burgoyne, J. Biol. Chem. 274 (1999) 30258–30265.
[21] K.B. Hendricks, B.Q. Wang, E.A. Schnieders, J. Thorner, Nat. Cell Biol. 1 (1999) 234–241.
[22] O. Pongs, J. Lindemeier, X.R. Zhu, T. Theil, D. Engelkamp, I. Krah-Jentgens, H.G. Lambrecht, K.W. Koch, J. Schwemer, R. Rivosecchi, A. Mallart, J. Galceran, I. Canal, J.A. Barbas, A. Ferrus, Neuron 11 (1993) 15–28.
[23] S. Matsuda, O. Hisatomi, T. Ishino, Y. Kobayashi, F. Tokunaga, J. Biol. Chem. 273 (1998) 20223–20227.
[24] C. Spilker, K. Richter, K.H. Smalla, D. Manahan-Vaughan, E.D. Gundelfinger, K.H. Braunewell, Neuroscience 96 (2000) 121–129.
[25] S. Saitoh, K. Takamatsu, M. Kobayashi, T. Noguchi, Neurosci. Lett. 157 (1993) 107–110.
[26] K. Takamatsu, T. Noguchi, Neurosci. Res. 17 (1993) 291–295.
[27] C.I. Seidenbecher, K. Langnaese, L. Sanmarti-Vila, T.M. Boeckers, K.H. Smalla, B.A. Sabel, C.C. Garner, E.D. Gundelfinger, M.R. Kreutz, J. Biol. Chem. 273 (1998) 21324–21331.
[28] N. Menger, C.I. Seidenbecher, E.D. Gundelfinger, M.R. Kreutz, Cell Tissue Res. 298 (1999) 21–32.
[29] A.M. Payne, S.M. Downes, D.A. Bessant, R. Taylor, G.E. Holder, M.J. Warren, A.C. Bird, S.S. Bhattacharya, Hum. Mol. Genet. 7 (1998) 273–277.
[30] T. Duda, R.M. Goraczniak, R.K. Sharma, Biochemistry 33 (1994) 7430–7433.

[31] I. Sokal, N. Li, I. Surgucheva, M.J. Warren, A.M. Payne, S.S. Bhattacharya, W. Baehr, K. Palczewski, Mol. Cell 2 (1998) 129–133.
[32] T.J. Schoenmakers, G.J. Visser, G. Flik, A.P. Theuvenet, Biotechniques 12 (1992) 870–879.
[33] M. Rudnicka-Nawrot, I. Surgucheva, J.D. Hulmes, F. Haeseleer, I. Sokal, J.W. Crabb, W. Baehr, K. Palczewski, Biochemistry 37 (1998) 248–257.
[34] A. Otto-Bruc, R.N. Fariss, F. Haeseleer, J. Huang, J. Buczylko, I. Surgucheva, W. Baehr, A.H. Milam, K. Palczewski, Proc. Natl. Acad. Sci. USA 94 (1997) 4727–4732.
[35] A. Mondragon, E.C. Griffith, L. Sun, F. Xiong, C. Armstrong, J.O. Liu, Biochemistry 36 (1997) 4934–4942.
[36] R. Roskoski Jr., Methods Enzymol. 99 (1983) 3–6.
[37] M.C. Posewitz, P. Tempst, Anal. Chem. 71 (1999) 2883–2892.
[38] R. Chattopadhyaya, W.E. Meador, A.R. Means, F.A. Quiocho, J. Mol. Biol. 228 (1992) 1177–1192.
[39] C.S. Ring, F.E. Cohen, FASEB J. 7 (1993) 783–790.
[40] L. Tabernero, D.A. Taylor, R.J. Chandross, M.F. Van Berkum, A.R. Means, F.A. Quiocho, J.S. Sack, Structure 5 (1997) 613–622.
[41] K.M. Flaherty, S. Zozulya, L. Stryer, D.B. McKay, Cell 75 (1993) 709–716.
[42] A.M. Dizhoor, S.G. Boikov, E. Olshevskaya, J. Biol. Chem. 273 (1998) 17311–17314.
[43] A. Ott-Bruc, J. Buczylko, I. Surgucheva, I. Subbaraya, M. Rudnicka-Nawrot, J. Crabb, A. Arendt, P.A. Hargrave, W. Baehr, K. Palczewski, Biochemistry 36 (1997) 4295–4302.
[44] K. Yamaguchi, F. Yamaguchi, O. Miyamoto, K. Sugimoto, R. Konishi, O. Hatase, M. Tokuda, J. Biol. Chem. 274 (1999) 3610–3616.
[45] C.B. Klee, M.H. Krinks, A.S. Manalan, P. Cohen, A.A. Stewart, Methods Enzymol. 102 (1983) 227–244.
[46] P.M. Stemmer, C.B. Klee, Biochemistry 33 (1994) 6859–6866.
[47] K.A. Peters, J.G. Demaille, E.H. Fischer, Biochemistry 16 (1977) 5691–5697.
[48] E.V. Olshevskaya, S. Boikov, A. Ermilov, D. Krylov, J.B. Hurley, A.M. Dizhoor, J. Biol. Chem. 274 (1999) 10823–10832.
[49] D.L. Garbers, D.G. Lowe, J. Biol. Chem. 269 (1994) 30741–30744.
[50] R.-B. Yang, D.C. Foster, D.L. Garbers, H.-J. Fülle, Proc. Natl. Acad. Sci. USA 92 (1995) 602–606.
[51] R.M. Goraczniak, T. Duda, R.K. Sharma, Biochem. Biophys. Res. Commun. 245 (1998) 447–453.
[52] F. Haeseleer, I. Sokal, N. Li, M. Pettenati, N. Rao, D. Bronson, R. Wechter, W. Baehr, K. Palczewski, J. Biol. Chem. 274 (1999) 6526–6535.
[53] T. Duda, R.M. Goraczniak, I. Surgucheva, M. Rudnicka-Nawrot, W.A. Gorczyca, K. Palczewski, A. Sitaramayya, W. Baehr, R.K. Sharma, Biochemistry 35 (1996) 8478–8482.
[54] R.P. Laura, A.M. Dizhoor, J.B. Hurley, J. Biol. Chem. 271 (1996) 11646–11651.
[55] A. Surguchov, J.D. Bronson, P. Banerjee, J.A. Knowles, C.C. Ruiz, I. Subbaraya, K. Palczewski, W. Baehr, Genomics 39 (1997) 312–322.
[56] J.B. Ames, A.M. Dizhoor, M. Ikura, K. Palczewski, L. Stryer, J. Biol. Chem. 274 (1999) 19329–19337.
[57] N. Pozdnyakov, Y. Yoshida, N.G.F. Cooper, A. Margulis, T. Duda, R.K. Sharma, A. Sitaramayya, Biochemistry 34 (1996) 14279–14283.
[58] V.D. Kumar, S. Vijay-Kumar, A. Krishnan, T. Duda, R.K. Sharma, Biochemistry 38 (1999) 12614–12620.
[59] S.M. Downes, G.E. Holder, F.W. Fitzke, A.M. Payne, M.J. Warren, S.S. Bhattacharya and A.C. Bird, Br. J. Ophthal. (2000) (submitted).
[60] E.V. Olshevskaya, A.N. Ermilov, A.M. Dizhoor, J. Biol. Chem. 274 (1999) 25583–25587.
[61] A. Nicholls, K.A. Sharp, B. Honig, Proteins 11 (1991) 281–296.